Chemical Science

RSC Publishing

EDGE ARTICLE

View Article Online
View Journal | View Issue



Cite this: *Chem. Sci.*, 2013, **4**, 4042

# $CO_2$ reduction by Fe(I): solvent control of C–O cleavage *versus* C–C coupling†

Caroline T. Saouma, Connie C. Lu,§ Michael W. Day‡ and Jonas C. Peters*

Received 7th May 2013
Accepted 11th July 2013

DOI: 10.1039/c3sc51262b

www.rsc.org/chemicalscience

This manuscript explores the product distribution of the reaction of carbon dioxide with reactive iron(I) complexes supported by tris(phosphino)borate ligands, $[PhBP^{R}_3]^-$ ($[PhBP^{R}_3]^- = [PhB(CH_2PR_2)_3]^-$; R = $CH_2Cy$, Ph, $^i$Pr, *m*ter; *m*ter = 3,5-*meta*-terphenyl). Our studies reveal an interesting and unexpected role for the solvent medium with respect to the course of the $CO_2$ activation reaction. For instance, exposure of methylcyclohexane (MeCy) solutions of $[PhBP^{CH_2Cy}_3]Fe(PR'_3)$ to $CO_2$ yields the partial decarbonylation product $\{[PhBP^{CH_2Cy}_3]Fe\}_2(\mu\text{-}O)(\mu\text{-}CO)$. When the reaction is instead carried out in benzene or THF, reductive coupling of $CO_2$ occurs to give the bridging oxalate species $\{[PhBP^{CH_2Cy}_3]Fe\}_2(\mu\text{-}\kappa OO'\text{:}\kappa OO'\text{-oxalato})$. Reaction studies aimed at understanding this solvent effect are presented, and suggest that the product profile is ultimately determined by the ability of the solvent to coordinate the iron center. When more sterically encumbering auxiliary ligands are employed to support the iron(I) center (*i.e.*, $[PhBP^{Ph}_3]^-$ and $[PhBP^{iPr}_3]^-$), complete decarbonylation is observed to afford structurally unusual diiron(II) products of the type $\{[PhBP^{R}_3]Fe\}_2(\mu\text{-}O)$. A mechanistic hypothesis that is consistent with the collection of results described is offered, and suggests that reductive coupling of $CO_2$ likely occurs from an electronically saturated "$Fe^{II}$–$CO_2^{\cdot-}$" species.

## I Introduction

Due to its vast supply, chemical versatility, and proposed role in global warming, $CO_2$ is poised as a C1 source for both fine chemicals and fuels;[1] several multi-electron transformations of $CO_2$ that effect its reduction to other C1 sources or create C–C bonds are feasible. For instance, the coupled two electron/two proton reduction of $CO_2$ to CO can serve as a chemical feedstock for CO, which can then be converted to liquid fuels *via* Fisher–Tropsch chemistry.[2] Examples of coupling reactions that involve $CO_2$ include cross-coupling with epoxides to generate polycarbonates or cyclic carbonates,[3] and coupling with organozinc or other carbanion equivalents to generate carboxylic acids.[4,5]

The aforementioned examples proceed *via* multi-electron transformations, but the direct one-electron reduction of $CO_2$ to give $CO_2^{\cdot-}$ can facilitate alternative reaction pathways. For instance, once formed, the $CO_2$ radical anion can disproportionate to CO and $CO_3^{2-}$,[6] it can generate formate in the presence of water,[7] it can cross-couple to other radicals,[8] or it can undergo C–C coupling to give oxalate.[9–14] The selective reduction of $CO_2$ to oxalate is a potentially desirable transformation, as oxalate can be hydrogenated to give ethylene glycol,[15] itself a useful fuel feedstock and gasoline additive. While trace oxalate formation has been observed in several electrocatalytic reduction systems,[16] well-defined homogeneous metal complexes that mediate reductive $CO_2$ coupling to oxalate remain rare. Evans and co-workers first reported that $Cp^*_2Sm(THF)_2$ reacts with $CO_2$ to produce the bridging oxalate species $\{Cp^*_2Sm\}_2(\mu\text{-}\kappa OO'\text{:}\kappa OO'\text{-oxalato})$,[9a] and subsequently there have been a few reports of similar transformations at lanthanides,[9b,c] copper,[10] nickel,[11] titanium,[14] and iron,[12,13] though how oxalate formation occurs in these systems is often ill-defined. Recently, a dimeric Cu(I) complex was found to mediate the selective reduction of $CO_2$ to oxalate at an unusually positive potential (relative to the 1-electron reduction of $CO_2$) when run electrocatalytically.[10b] These results underscore and lend motivation to the need for establishing well-defined systems that selectively reduce $CO_2$, and to understanding key factors that dictate the product profile.

Our group previously described an Fe(I)-mediated reduction of $CO_2$ in which a bridging oxalate species was formed as a minor product (Scheme 1).[12] The iron(I) synthon $[PhBP^{CH_2Cy}_3]Fe$ (**1**) reduced $CO_2$ to generate blue-green and diamagnetic $\{[PhBP^{CH_2Cy}_3]Fe\}_2(\mu\text{-}O)(\mu\text{-}CO)$ (**2**) as the major product of a partial decarbonylation reaction. A red and paramagnetic bridging

*California Institute of Technology, Division of Chemistry and Chemical Engineering, Pasadena, California, 91125, USA. E-mail: jpeters@caltech.edu*

† Electronic supplementary information (ESI) available: Experimental procedures, UV-Vis spectra of **1** and **8**, X-band EPR spectrum of **1** in MeCy, $^1$H NMR profile of the reaction between **12** and $CO_2$, 50% thermal ellipsoid representation of **14**, and DFT details. CCDC 604498, 605316, 626195 and 937863–937865. For ESI and crystallographic data in CIF or other electronic format see DOI: 10.1039/c3sc51262b

‡ Deceased.

§ Current address: University of Minnesota, Department of Chemistry, Minneapolis, Minnesota, 55455, USA.

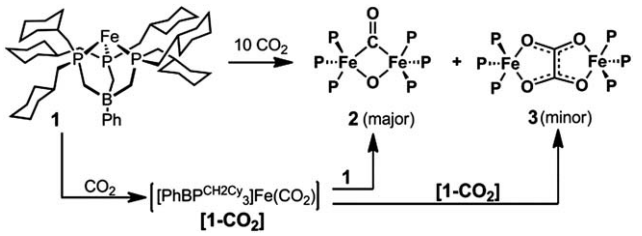


**Scheme 1** Starting mechanistic hypothesis for the reaction of **1** with $CO_2$.

oxalate species, $\{[PhBP_3^{CH_2Cy}]Fe\}_2(\mu\text{-}\kappa OO'\text{:}\kappa OO'\text{-oxalato})$ (**3**), was formed as a minor C–C coupling product in an approximately 1 : 3 ratio of **3 : 2** ($[PhBP_3^{CH_2Cy}]^- = PhB(CH_2P(CH_2Cy)_2)_3^-$). To our knowledge, this iron(I) system is the only molecular system that displays the aforementioned dual reactivity, that is, $CO_2$ decarbonylation and C–C coupling. We thereby sought to establish the dominant factors that dictate the selectivity profile. In brief, we now show that reductive coupling to oxalate can be favoured with the "$[PhBP_3^{CH_2Cy}]Fe(I)$" platform and that this $CO_2$-coupling product is preferred in a solvent that can coordinate the iron center. Thus, in THF $CO_2$ coupling to μ-oxalate **3** is favoured, whereas in methylcyclohexane (MeCy) partial decarbonylation to generate μ-O/μ-CO **2** occurs exclusively.

# II Results

## II.1 Initial observations

Following on our original report,[12] attempts to alter the product profile between **1** and $CO_2$ to favour the C–C coupling product **3** initially focused on systematically varying the ratio of $CO_2$ equivalents and the initial concentration of **1** (*ca.* 10 mM) in solution.[12] When a sample of **1** in THF (11 mM) was further diluted in pentane to 0.03 mM, and subsequently exposed to an atmosphere of $CO_2$ (*ca.* 300 equiv., 0.03 M), the selectivity changed to favour the oxalate product **3**. This result appeared to us consistent with the mechanistic outline presented in Scheme 1. If enough $CO_2$ is present to efficiently tie up **1** in the form of an intermediate $CO_2$ adduct species, $[PhBP_3^{CH_2Cy}]Fe(CO_2)$ (**1**-$CO_2$), then bimolecular C–C coupling by **1**-$CO_2$ to afford μ-oxalate **3** is favoured. Otherwise **1** remains available to intercept **1**-$CO_2$ to generate μ-O/μ-CO **2** as the dominant product. The ratio of **1** *vs.* **1**-$CO_2$ at a given time in the reaction course dictates the product selectivity.

To achieve selectivity for either formation of **2** or **3**, two synthetic strategies were subsequently implemented. First, various four-coordinate iron(I) phosphine adducts of the type $[PhBP_3^{CH_2Cy}]Fe(PR'_3)$ were prepared and their reactivity with $CO_2$ canvassed. Because it was anticipated that phosphine dissociation would precede binding of $CO_2$, this approach would allow the concentration of the active iron(I) species in solution to be kept low relative to the concentration of $CO_2$ in solution, but would not require high dilution conditions (thus increasing the relative concentration of **1**-$CO_2$ *vs.* **1**). High dilution of **1** proved empirically problematic with regard to obtaining a clean product profile, owing to the high reactivity of **1**. Second, the *in situ* generation of iron(I) in the presence of an atmosphere of $CO_2$ was explored using several $[PhBP_3^R]^-$ ligands.

## II.2 Synthesis and characterization of iron(I) species

In our initial report,[12] it was noted that the sodium amalgam reduction of $[PhBP_3^{CH_2Cy}]FeCl$ in THF produced a species whose empirical formula, in the solid state, proved to be "$[PhBP_3^{CH_2Cy}]Fe$" (**1**). Dissolution of **1** in THF produces a lime-green equilibrium mixture of isomers (collectively referred to as **1**), which include species of the type $[PhBP_3^{CH_2Cy}]Fe(THF)_x$. As a temperature dependent $^{31}P$ NMR signal centred at −25 ppm is observed for **1** in $d_8$-THF, one of these species is presumed to be $\{\kappa^2\text{-}[PhBP_3^{CH_2Cy}]\}Fe(THF)_x$, in which one of the phosphine arms has dissociated (Scheme 2). Despite this equilibrium mixture of species, **1** behaves as a clean iron(I) synthon in THF, for example, on reaction with phosphines (Scheme 2) or organic azides.[12]

To simplify the characterization of this species, spectroscopic data for **1** have now been collected in MeCy, whose non-coordinating nature should lead to a structure analogous to that in the solid state. Our data are most consistent with its formulation as the cyclometalated iron(III) hydride complex depicted in Scheme 2 (where the exact position of metalation on the ring remains unclear), which may be in further equilibrium with a 3-coordinate Fe(I) species. Relevant data supporting the former assignment are as follows: powders, as well as MeCy solutions of **1**, are yellow in colour, whereas they are lime-green in a donor solvent such as THF (see ESI†). Also, a low intensity but reliably discernible $\nu$(Fe–H) vibration is present in MeCy (2056 $cm^{-1}$) and in the solid state (2058 $cm^{-1}$; KBr), but absent in THF solutions. Both the EPR spectrum of **1** in MeCy at 4 K (see ESI†), as well as the room temperature $d_{14}$-MeCy solution magnetic moment of 2.3 $\mu_B$, are consistent with an $S = ½$ spin system. Finally, as noted above for THF solutions of **1**, the addition of phosphines to **1** in MeCy leads to formation of the corresponding $d^7$ $S = 3/2$ $[PhBP_3^{CH_2Cy}]Fe(PR'_3)$ complexes (*vide infra*), consistent with a reversible cyclometalation process.

Upon addition of 0.5 equiv. of benzene to THF solutions of **1**, quantitative coordination of benzene occurs to generate the benzene-bridged diiron complex $\{[PhBP_3^{CH_2Cy}]Fe\}_2(\mu\text{-}\eta^3\text{:}\eta^3\text{-}C_6H_6)$ (**4**) (Scheme 2). Whereas we have been unable to obtain crystals of **1** suitable for X-ray diffraction studies from MeCy or THF, the structure of **4**, which is a bridged benzene adduct complex that is presumably formed by reaction of "$[PhBP_3^{CH_2Cy}]Fe(benzene)$" with **1**, has been obtained and is shown in Fig. 1a.[12] The solid-state structure of **4** reveals an average C–C bond distance for the bound benzene ring of 1.40 Å, with the C52–C54 distance being larger than that of C53–C54 or C52–C53′ (Fig. 1a and caption). Also, a relatively small average dihedral angle (between the planes defined by the benzene C atoms) of *ca.* 12° distorts the coordinated benzene molecule into a pseudo-chair conformation.[17] In solution, complex **4** is diamagnetic, and the benzene protons appear as a single sharp resonance at 4.91 ppm in the $^1H$ NMR spectrum.

In the presence of excess benzene, **4** is thermally unstable and decomposes at 25 °C to give the 18-electron dimeric product, $\{[PhBP_3^{CH_2Cy}]Fe\}(\mu\text{-}\eta^5\text{:}\eta^5\text{-}6,6'\text{-bicyclohexadienyl})$ (**5**) (Scheme 2 and Fig. 1b). The transformation from **4** to **5** presumably results from the dimerization of a formally

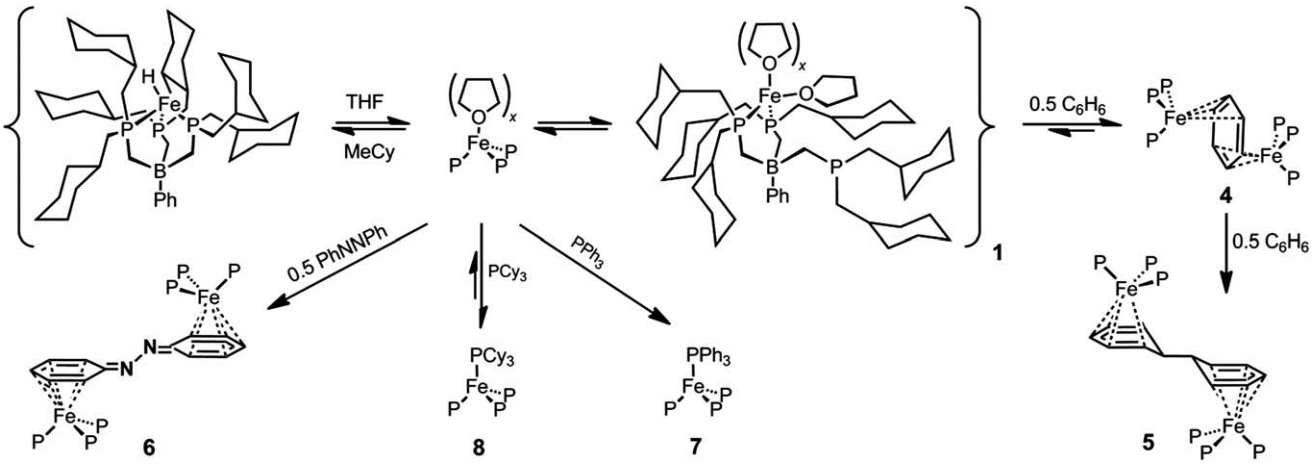


Scheme 2

19-electron intermediate species, "$\{[PhBP_3^{CH_2Cy}]Fe\}_2(\eta^6\text{-}C_6H_6)$", that then undergoes radical C–C coupling between the two activated benzene ligands (due to substantial spin leakage onto the bound arene ring).[18] This reaction is reminiscent of other ligand-based reductive C–C coupling reactions reported for Ru,[19] Fe,[20] and Co.[21]

To probe the lability of the bound benzene in **4**, a $C_6D_6$ solution of $\{[PhBP_3^{CH_2Cy}]Fe\}_2(\mu\text{-}\eta^3\text{:}\eta^3\text{-}C_6H_6)$ was heated to 50 °C. By $^{31}P$ NMR spectroscopy, full conversion to **5** was observed after 8 h. By $^1H$ NMR spectroscopy, the signal for the bound bicyclohexadienyl group was completely absent, indicating that benzene exchange had occurred. To probe whether this exchange occurred in **4** or **5**, a $C_6D_6$ solution of **5** was heated to 100 °C for 72 h. The $^1H$ NMR signals for the bicyclohexadienyl group were retained, establishing that benzene exchange occurred in **4**, and that the newly formed C–C bond in **5** was not reversibly cleaved. This contrasts the reversible radical C–C bond formation observed in related iron systems that couple pyridine[20b] or azaallyl[20a] ligands. Though the coordination of benzene in **4** is reversible, the subsequent dimerization reaction makes **4** unsuitable as an iron(I) synthon for reactivity studies with $CO_2$.

In a conceptually related reaction, **1** reacts with 0.5 equiv. of azobenzene (Scheme 2) to generate $\{[PhBP_3^{CH_2Cy}]Fe\}_2(\mu\text{-}\eta^5\text{:}\eta^5\text{-azobenzene})$ (**6**). The solid-state structure of **6** shows, what is to our knowledge, an unprecedented binding mode for aryl-substituted diazenes (Fig. 1c). Instead of coordinating the nitrogen atom(s),[22,23] the iron centres are bound by the aryl rings in an $\eta^5$-fashion, structurally akin to the arene binding mode of **5**. The N–N bond distance in **6** is 1.340(9) Å, which is significantly elongated compared to that of free azobenzene, wherein the N=N bond distance is 1.23 Å.[24] This suggests that the N=N bond of azobenzene in **6** has been reduced by two electrons, implying the presence of two 18-electron iron(II) centres. The relatively poor quality of the structure of **6** warrants a degree of caution with regard to this interpretation.

Access to well-defined and less reactive iron(I) complexes is achieved by the preparation of four-coordinate species of the type $[PhBP_3^{CH_2Cy}]Fe(PR'_3)$. These complexes are readily synthesized by the addition of a suitable phosphine to THF or MeCy solutions of **1** (Scheme 2). For example, the addition of $PPh_3$ to a THF solution of **1** results in a rapid colour change from lime-green to dark orange, and quantitative formation of four-coordinate $S = 3/2[PhBP_3^{CH_2Cy}]Fe(PPh_3)$ (**7**).[12,25,26]

In contrast, the addition of one equivalent of bulkier $PCy_3$ to a solution of **1** results in an equilibrium between **1** and $[PhBP_3^{CH_2Cy}]Fe(PCy_3)$ (**8**), as determined by UV-Vis absorption spectroscopy (Scheme 2 and ESI†). The addition of one equivalent of $PCy_3$ to **1** gives an equilibrium mixture at room temperature in which *ca.* 57% of the $PCy_3$ is tied up to give **8** in THF, *versus ca.* 95% in MeCy (*ca.* 0.5 mM **1**). The similar solution magnetic moments obtained for **7** (4.2 $\mu_B$) and **8** (3.9 $\mu_B$) in

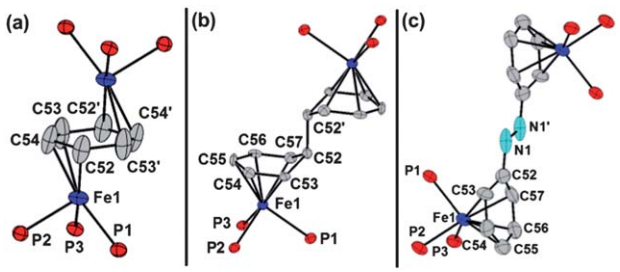


**Fig. 1** 50% thermal ellipsoid representation of the core atoms of: (a) $\{[PhBP_3^{CH_2Cy}]Fe\}_2(\mu\text{-}\eta^3\text{:}\eta^3\text{-}C_6H_6)$ (**4**), (b) $\{[PhBP_3^{CH_2Cy}]Fe\}_2(\mu\text{-}\eta^5\text{:}\eta^5\text{-}6,6'$-bicyclohexadienyl) (**5**), and (c) $\{[PhBP_3^{CH_2Cy}]Fe\}_2(\mu\text{-}\eta^5\text{:}\eta^5\text{-azobenzene})$ (**6**). Hydrogen atoms have been omitted for clarity. Select bond distances (Å) and angles (deg.) for **4**: Fe1–P1 2.234(2), Fe1–P2 2.231(2), Fe1–P3 2.268(2) Fe1–C52 2.219(5), Fe1–C53 2.234(5), Fe1–C54 2.169(5), C53–C54 1.385(5), C54–C52 1.420(5), C52–C53′ 1.384(5), C52–C53′-C54′–C52′ dihedral 12.84(1). Select bond distances (Å) and angles (deg.) for **5**: Fe1–P1 2.262(2), Fe1–P2 2.235(2), Fe1–P3 2.250(2), Fe–C53 2.174(5), Fe–C54 2.100(5), Fe–C55 2.112(5), Fe–C56 2.103(5), Fe–C57 2.188(5), C52–C52′ 1.56(1), C54–C53–C52–C57 dihedral 50.25(1). Select bond distances (Å) for **6**: Fe1–P1 2.250(2), Fe1–P2 2.230(2), Fe1–P3 2.246(2), Fe1–C53 2.238(6), Fe1–C54 2.094(6), Fe1–C55 2.089(6), Fe1–C56 2.110(6), Fe1–C57 2.212(6), N1–C52 1.429(8), N1–N1′ 1.340(9).

$C_6D_6$ and THF-$d_8$, respectively, confirms that at *ca.* 10 mM solutions in THF, most of the $PCy_3$ is tied up in **8**. Were this not so, a lower solution magnetic moment would be anticipated, as the 4-coordinate phosphine adducts are $S = 3/2$, and **1** is $S = ½$. The lability of $PCy_3$ manifests itself in the instability of **8** towards arene solvents. For instance, whereas benzene solutions of $PPh_3$-capped **7** are stable over a period of weeks, a $C_6D_6$ solution of **8**, generated by dissolution of solid **1** and one equiv. of $PCy_3$ in $C_6D_6$, shows full conversion to the diiron-bridged benzene complex **4**-$d_6$ after a period of hours (as monitored by $^1$H and $^{31}$P NMR spectroscopy). Additionally, cooling THF or MeCy solutions of **8** results in respective colour changes to lime-green or yellow, as $PCy_3$ precipitates and **1** is liberated into solution.

### II.3 Reaction of $[PhBP_3^{CH_2Cy}]Fe(I)$ complexes with $CO_2$

As originally reported,[12] when solutions of **1** (*ca.* 10 mM) in either THF or MeCy are exposed to 10 equiv. of $CO_2$, the partial decarbonylation pathway to generate μ-O/μ-CO **2** predominates over the coupling pathway to generate μ-oxalate **3**, with an *ca.* 3 : 1 distribution of **2** to **3** (Scheme 1). To decrease the concentration of reactive **1** in solution relative to $CO_2$, the four-coordinate phosphine complexes were instead exposed to $CO_2$.

Treatment of a benzene solution of $PPh_3$-adduct **7** to $CO_2$ (one atm) results in a change in colour from dark orange to dark red, and both NMR and IR analysis show a clean, albeit incomplete, conversion to the bridging oxalate product **3** over a period of 26 h (Scheme 3). When the reaction is monitored by $^{31}$P NMR spectroscopy, a broad but discernible resonance is observed at 45 ppm at intermediate reaction times, consistent with the presence of the diiron bridged benzene complex **4** in solution; subsequent formation of **5** *via* benzene coupling is not observed. A typical experiment (15 mM in **7**, 10 equiv. or *ca.* 0.14 M $CO_2$, 26 h) gives rise to *ca.* 70% **3**, with *ca.* 30% of the starting material remaining (see Experimental section of ESI for details concerning the quantification method†). Exposure of such solutions to additional $CO_2$ with prolonged stirring does not completely convert the $PPh_3$-adduct **7** to μ-oxalate **3**, suggesting that the gradual release of $PPh_3$ has an inhibitory effect on the reaction. Indeed, when excess $PPh_3$ (10-fold) is added to solutions of **7** prior to $CO_2$ exposure, the reaction is completely shut down at room temperature. In THF, a similar selectivity is observed, though after 26 h only 30% conversion to **3** is observed.

By contrast, when the reaction between **7** and $CO_2$ is carried out in MeCy, a sharp attenuation in rate and *complete inversion* of selectivity is observed. The partial decarbonylation product **2** is now produced *exclusively* after a period of 26 h at 50 °C, albeit in low yield (*ca.* 10%), with the remaining iron present as starting material. The variable inhibitory effect that $PPh_3$ has on the reaction in the various solvents is presumably due to solvent-dependent equilibria between **1** and **7**.

Similarly, the reaction between the dinuclear benzene adduct **4** and $CO_2$ displays the same solvent-dependence, though as noted above, the competitive conversion of **4** to **5** precludes a thorough study using this iron(I) synthon.

To further probe the role that solvent plays on the product profile, the reaction between $PCy_3$-adduct **8** and $CO_2$ was next investigated. Under similar conditions, the reactions of **7** and **8** towards $CO_2$ give similar product distributions, though the latter reactions are complete after 24 h. For these studies, solutions of **8** were prepared by the addition of one equiv. of $PCy_3$ to **1** (20 mM) followed by exposure to ten equiv. (0.19 M) of $CO_2$ for 24 h (Scheme 4 and Table 1). We sought a means to readily discern the ratio between μ-O/μ-CO **2** and μ-oxalate **3**, which is non-trivial by NMR spectroscopy owing to the paramagnetism of **3**. The following viable protocol was established: after the reaction with $CO_2$ was complete, the reaction headspace was evacuated, and an atmosphere of CO was introduced. The addition of CO served to quantitatively convert the μ-oxalate complex **3** to its diamagnetic carbonyl adduct **9**, $\{[PhBP_3^{CH_2Cy}]Fe(CO)\}_2$(μ-κOO′:κOO′-oxalato) while not affecting the partial decarbonylation product **2** (Scheme 4). In the control reaction, whereby an atmosphere of CO was added to a solution of **2**, no reaction ensued, as ascertained by $^1$H and $^{31}$P NMR and IR spectroscopies. The complex $\{[PhBP_3^{CH_2Cy}]Fe(CO)\}_2$(μ-κOO′:κOO′-oxalato) was originally identified in trace amounts solely by X-ray crystallography,[12] but has now been independently synthesized and thoroughly characterized (see ESI†). This protocol allows for the direct quantification of **2** *versus* **9** in solution by $^{31}$P NMR spectroscopy, thus permitting the relative rates of formation of **2** *versus* **3** to be obtained.

Under the aforementioned conditions, the only observable product in MeCy is that of partial decarbonylation, **2** (Table 1, entries 1–3). This is also true if less $CO_2$ is administered (2 equiv.), or if 5 equiv. of $PCy_3$ is added to the reaction, though in these latter cases incomplete conversion to **2** is observed after 24 h. If THF is employed as the solvent rather than MeCy, **8** reacts under analogous conditions to instead favour μ-oxalate **3** (entries 4–6). If the $CO_2$ content is reduced to 2 equiv., a ratio of 13 : 1 in favour of **3** (*versus* **2**) is observed in THF. The addition of excess $PCy_3$ also increases the selectivity for **3**.

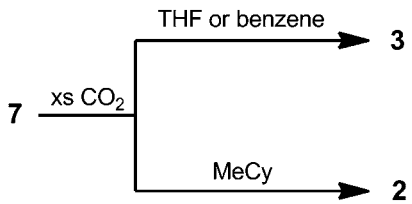


**Scheme 3** Solvent dependence of the reaction of **7** with $CO_2$.

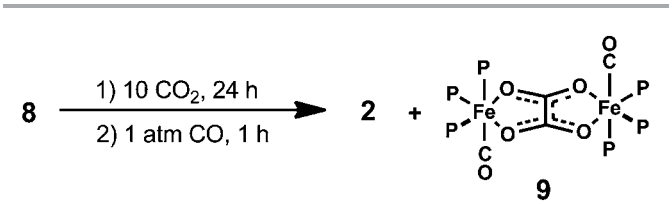


**Scheme 4**

**Table 1** Reactivity of **8** (20 mM) towards $CO_2$, as depicted in Scheme 4

| Entry | Solvent | $CO_2$ equiv.[a] (molarity) | Equiv. (molarity) additives | **2 : 3**[b] |
|---|---|---|---|---|
| 1 | MeCy | 10 (0.19) | — | 1 : 0 |
| 2 | MeCy | 10 (0.19) | 5 (0.08) $PCy_3$ | 1 : 0 |
| 3 | MeCy | 2 (0.034) | — | 1 : 0 |
| 4 | THF | 10 (0.19) | — | 1 : 4.3 |
| 5 | THF | 10 (0.19) | 5 (0.08) $PCy_3$ | 1 : 9 |
| 6 | THF | 2 (0.030) | — | 1 : 13 |
| 7 | 2-MeTHF | 2 (0.030) | — | 1 : 7 |
| 8 | 2,5-DiMeTHF | 2 (0.030) | — | 4 : 1 |

[a] The molarity of $CO_2$ in solutions was estimated using the Henry's law constant of 84.0 $atm^{-1}$ for $^n$heptane (as an estimate for the solubility in MeCy) and of 44.9 $atm^{-1}$ for THF (for the solubility in THF and an estimate for the solubility in 2-MeTHF, and 2,5-diMeTHF).[27] [b] The ratio **2 : 3** was determined by $^{31}$P NMR integration of resonances associated with **2** and **9** against an internal standard of $^t$$Bu_3$P (see Experimental section of ESI and text for details).

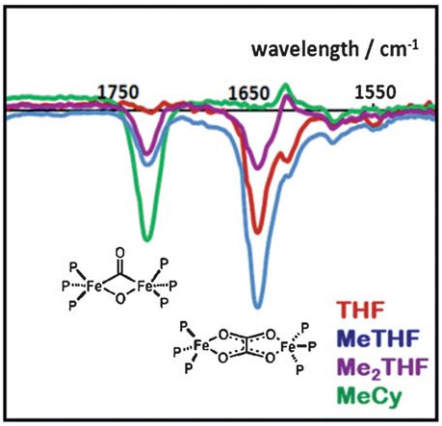


**Fig. 2** Stacked IR spectra ($KBr/C_6D_6$) of the reaction between **8** and 10 equiv. $CO_2$ in various solvents. The IR spectra were taken prior to CO addition. The $\nu$(CO) for **2** at 1730 $cm^{-1}$ is less intense than the $\nu$(oxalate) for **3** at 1644 $cm^{-1}$.

The reaction between $PCy_3$-adduct **8** and $CO_2$ was examined in 2-methyl-THF and 2,5-dimethyl-THF.[28] These two solvents have dielectric constants very similar to THF,[29] yet the added steric bulk renders them less coordinating than THF, 2,5-dimethyl-THF being the most distinct in this regard.

In 2-methyl-THF, as for THF, the major product remains the μ-oxalate species **3**, though the amount of μ-O/μ-CO **2** produced increases relative to when the reaction is run in THF (Table 1 and Fig. 2). For 2,5-dimethyl-THF, the selectivity *inverts* (4 : 1 in favour of **2**), better reproducing the selectivity observed in MeCy. The implication of these results is clear: a more coordinating solvent favours C–C coupling.

### II.4 Reaction between *in situ* generated iron(I) and $CO_2$

The role that the auxiliary $[PhBP_3^R]^-$ ligand plays on the outcome of the reaction between iron(I) and $CO_2$ was explored by comparing the product profiles of the *in situ* reductions of $[PhBP_3^R]FeCl$ in the presence of $CO_2$. This approach was sought as the phosphine adducts $[PhBP_3^{iPr}]Fe(PMe_3)$[26a] and $[PhBP_3^{Ph}]Fe(PPh_3)$[25] do not react readily with $CO_2$ (1 atm, RT), precluding a direct comparison to the reactions of $[PhBP_3^{CH_2Cy}]Fe(PR'_3)$ with $CO_2$. Because it is known that the Na/Hg reductions of $[PhBP_3^R]FeCl$ (R = $^i$Pr, MeCy) readily occur in THF,[12,30] and that all Fe species considered are soluble in THF, these studies were exclusively conducted in THF.

*In situ* Na/Hg reductions of $[PhBP_3^R]FeCl$ under a $CO_2$ atmosphere (R = $CH_2Cy$, $^i$Pr, Ph, *m*ter) were canvassed as a means to slowly introduce iron(I) in solution. In a typical experiment, an atmosphere of $CO_2$ was introduced to an evacuated reaction vessel containing 2.5 equiv. of Na/Hg and a THF solution of $[PhBP_3^R]FeCl$ at 0 °C. The solution was slowly stirred to ensure a large excess of $CO_2$ in solution relative to iron(I) (Scheme 5).

When $[PhBP_3^{CH_2Cy}]FeCl$ is employed as the Fe source, μ-oxalate **3** is isolated as the major species (50%), with no observable formation of **2** (as deduced by NMR and IR spectroscopy). The remainder of the iron is converted to unidentifiable products. As reducing amalgams can themselves reductively couple $CO_2$ to give oxalate salts,[31] it is conceivable that **3** forms from the reaction between sodium oxalate and $[PhBP_3^{CH_2Cy}]FeCl$. In a control experiment, no reaction between $[PhBP_3^{CH_2Cy}]FeCl$ and sodium oxalate under similar conditions (*i.e.*, 0 °C, THF) is observed, as ascertained by NMR and IR spectroscopy. This is true when either crystalline sodium oxalate or *in situ* generated sodium oxalate (prepared by stirring a sodium amalgam suspended in THF under a blanket of $CO_2$) is employed. Thus, **3** presumably forms from the reaction between **1** and $CO_2$.

By contrast, the reduction of $[PhBP_3^{iPr}]FeCl$[32] under an atmosphere of $CO_2$ leads to *complete* rather than partial decarbonylation (Scheme 5), and mixtures containing a large amount of $\{[PhBP_3^{iPr}]Fe\}_2(\mu\text{-}O)$ (**10**) and $[PhBP_3^{iPr}]Fe(CO)_2$ (**11**) are observed, amongst other unidentified products. Whereas these reactions are reproducible in that **10** and **11** are always observed,

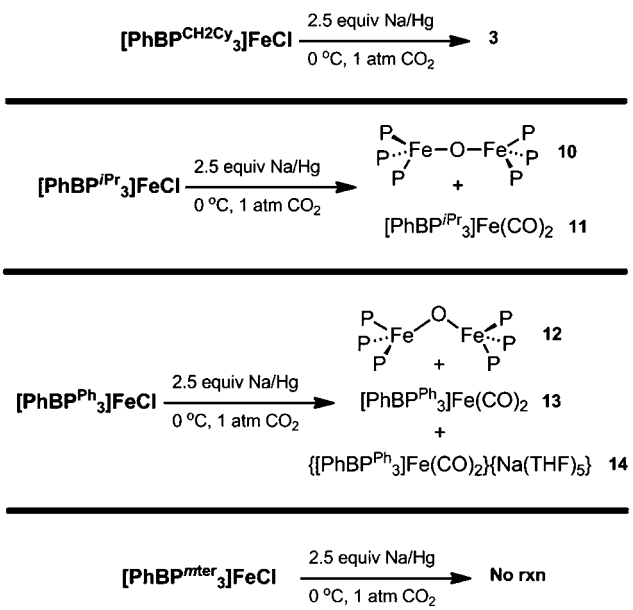


**Scheme 5**

the product distributions vary between independent runs. Similar disparities in the product profile are also observed in the reaction between the well-defined iron(I) source $\{[PhBP_3^{iPr}]Fe\}_2(\mu\text{-}N_2)$ and $CO_2$.

The difficulty in reproducing the product distributions may indicate that the initial product(s) formed from the reaction of iron(I) and $CO_2$ further react with either CO or $CO_2$. Indeed, subsequent exposure of isolated $Fe_2(\mu\text{-}O)$ **10** to one equiv. of either CO or $CO_2$ at −78 °C gives rise to incomplete conversion to several products, many of which correlate to the spectroscopically observed, but unidentified, products in the aforementioned reaction.

The *in situ* reduction of $[PhBP_3^{Ph}]FeCl$[25] under an atmosphere of $CO_2$ likewise results in complete decarbonylation, generating $\{[PhBP_3^{Ph}]Fe\}_2(\mu\text{-}O)$ (**12**), $[PhBP_3^{Ph}]Fe(CO)_2$ (**13**),[25] and $\{[PhBP_3^{Ph}]Fe(CO)_2\}\{Na(THF)_5\}$ (**14**), as depicted in Scheme 5. This reaction is much cleaner and the product profile is more reproducible than that described above for the "$[PhBP_3^{iPr}]Fe$(I)" system.

Exposure of $Fe_2(\mu\text{-}O)$ **12** to CO affords dicarbonyl **13**, as ascertained by $^1$H NMR and IR spectroscopies. Production of $CO_2$ as a possible by-product was not confirmed. Also, $CO_2$ reversibly inserts into the Fe–O bond of **12** to generate the paramagnetic, bridging carbonate complex $\{[PhBP_3^{Ph}]Fe\}_2(\mu\text{-}\eta^2\text{:}\eta^1\text{-}CO_3)$ (**15**). This reaction requires prolonged stirring at room temperature (days) or heating to 60 °C for 1 hour. Curiously, **15** appears to liberate $CO_2$ and regenerate **12** to some extent under vacuum (see ESI†).[33] Crystals of **15** could nonetheless be grown and its solid-state structure establishes the presence of a bridging carbonate (Fig. 3c).

The *in situ* reduction of the highly sterically encumbered precursor $[PhBP_3^{mter}]FeCl$[34] under a $CO_2$ atmosphere was canvassed and afforded no net reaction: $[PhBP_3^{mter}]FeCl$ is the only iron containing species observed by $^1$H and $^{31}$P NMR and IR spectroscopies.

In the combined *in situ* reductions of $[PhBP_3^{R}]FeCl$ under a $CO_2$ atmosphere (R = $^i$Pr, Ph, *m*ter), no stretches that would correspond to an iron oxalate are observed by IR spectroscopy (sodium oxalate is observed in all of these reactions).[35] Thus, reductive coupling of $CO_2$ to oxalate at tris(phosphino)borate supported iron(I) only occurs when the iron is supported by the $[PhBP_3^{CH_2Cy}]^-$ ligand scaffold. Moreover, this ligand scaffold gives rise to the diiron μ-O/μ-CO structure type, which to our knowledge, remains the only species to exhibit an $M_2(\mu\text{-}O)(\mu\text{-}CO)$ core.

### II.5 Structural data for $Fe_2^{II}(\mu\text{-}O)$ complexes 10 and 12

The μ-O species **10** and **12** are unusual in that they are rare examples of the diferrous bridging oxo motif, $Fe_2^{II}(\mu\text{-}O)$, the only other example being that reported by Holland's lab, $\{L^{tBu}Fe\}_2(\mu\text{-}O)$ ($L^{tBu}$ = ArNC($^t$Bu)CHC($^t$Bu)Ar$^-$, Ar = 2,6-diisopropylphenyl).[36] While the solid-state structure of **10** is of comparatively poor quality (see ESI†), structural differences can be summarized as follows: the phosphines are eclipsed in **12** and staggered in **10**, and each iron center in **10** has one long and two short Fe–P bonds, whereas all three Fe–P bond distances are similar in **12**. Most notably, the bridging oxo is nearly linear in **10** (175°), whereas it is bent in **12** (148°), the latter of which is reminiscent of the related nitrido species, $\{[PhBP_3^{Ph}]Fe\}_2(\mu\text{-}N)^-$ (Fe–N–Fe: 135.9(3)°).[37] Despite these differences, both **10** and **12** have a similar room temperature solution magnetic susceptibility (*ca.* 2.8 $\mu_B$). The low magnetic susceptibility, combined with the long Fe–P bond distances,[12,25,32] suggest that there is moderately strong antiferromagnetic coupling between two high-spin iron centres in both **10** and **12**.

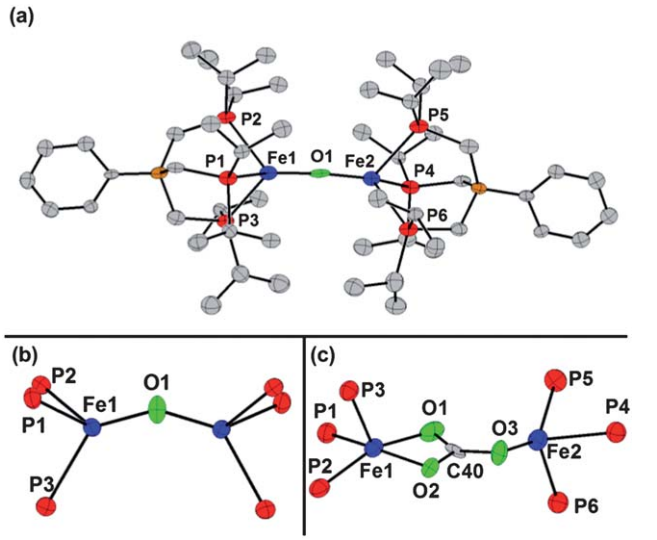


**Fig. 3** 50% thermal ellipsoid representation of (a) $\{[PhBP_3^{iPr}]Fe\}_2(\mu\text{-}O)$ (**10**), (b) the core atoms of $\{[PhBP_3^{Ph}]Fe\}_2(\mu\text{-}O)$ (**12**), and (c) the core atoms of $\{[PhBP_3^{Ph}]Fe\}_2(\mu\text{-}\eta^2\text{:}\eta^1\text{-}CO_3)$, (**15**). Hydrogen atoms, solvent molecules, and minor components of disorder are omitted for clarity. See ESI for complete details.†

## III Discussion

### III.1 Role of the auxiliary $[PhBP_3^{R}]^-$ ligand in $CO_2$ reduction

Whereas μ-oxalate **3** is the major product in the *in situ* reduction of $[PhBP_3^{CH_2Cy}]FeCl$ with $CO_2$, complete decarbonylation to give $Fe_2(\mu\text{-}O)$ **10** and dicarbonyl **11** is observed in the analogous reduction of $[PhBP_3^{iPr}]FeCl$ (Scheme 5). Likewise, complete decarbonylation is exclusively observed upon reduction of $[PhBP_3^{Ph}]FeCl$ under $CO_2$.

Electronic factors do not appear to dominate the product selectivity. In accord with this notion, the $[PhBP_3^{CH_2Cy}]Fe$- and $[PhBP_3^{iPr}]Fe$-systems show very similar quasi-reversible reduction potentials for their respective chlorides $[PhBP_3^{R}]FeCl$ (−1.94 and −2.03 V *vs.* Fc/Fc$^+$),[12,32] whereas the couple for $[PhBP_3^{Ph}]FeCl$ is shifted anodically by *ca.* 300 mV (−1.61 V *vs.* Fc/Fc$^+$).[25] In addition, both $[PhBP_3^{CH_2Cy}]Fe(CO)_2$ and $[PhBP_3^{iPr}]Fe(CO)_2$ have very similar $\nu$(CO) stretches (1959/1894 cm$^{-1}$ and 1955/1888 cm$^{-1}$, respectively) that are substantially lower in energy than those for $[PhBP_3^{Ph}]Fe(CO)_2$ (1979/1914 cm$^{-1}$).[25] That the $[PhBP_3^{Ph}]Fe$- and $[PhBP_3^{iPr}]Fe$-systems give similar product profiles that are unique from that of the $[PhBP_3^{CH_2Cy}]Fe$-system argues against an electronic cause.

A qualitative comparison of the steric profiles of the three $[PhBP_3^{R}]Fe$-systems in the vicinity of the Fe center can be

gleaned from their comparative accessibilities to the phosphine adduct complexes $[PhBP_3^R]Fe(PR'_3)$, where the R′ group of the $PR'_3$ ligand is varied from Me to Ph to Cy (cone angles corresponding to 118, 145, and 170°).[38] $[PhBP_3^{CH_2Cy}]Fe(PR'_3)$ complexes can be generated for all three phosphines, whereas $[PhBP_3^{Ph}]Fe(PR'_3)$ complexes are available for R = Me and Ph, and $[PhBP_3^{iPr}]Fe(PR'_3)$ is only accessible for R = Me. Based on this information, the steric profiles of the three systems can be ordered as follows: $[PhBP_3^{CH_2Cy}]Fe < [PhBP_3^{Ph}]Fe < [PhBP_3^{iPr}]Fe$. It is these relative steric profiles that we suggest dominates the $CO_2$ reduction product selectivity.

The partial decarbonylation product $Fe_2(\mu\text{-}O)(\mu\text{-}CO)$ is only observed for the $[PhBP_3^{CH_2Cy}]Fe$-system (complex **2**). The structure of this complex reveals a short Fe–Fe distance of 2.384(4) Å, and this distance requirement likely destabilizes such a product for the sterically more crowded $[PhBP_3^{Ph}]Fe$- and $[PhBP_3^{iPr}]Fe$-systems. As we will further suggest below, we also suspect that the more crowded $[PhBP_3^{Ph}]Fe$- and $[PhBP_3^{iPr}]Fe$-systems disfavour access to coordinatively saturated and 19-electron "$[PhBP_3^R]Fe(solv.)_2(CO_2)$" complexes that proceed along a C–C coupling pathway to generate oxalate (solv. = solvent). Hence no oxalate is observed for these systems, again contrasting the $[PhBP_3^{CH_2Cy}]Fe$-system (complex **3**).

The very encumbered 3,5-*meta*-terphenyl system $[PhBP_3^{mter}]$-Fe affords a much deeper binding pocket than for $[PhBP_3^R]Fe$-systems (R = $CH_2Cy$, $^i$Pr, Ph), while maintaining a similar electronic environment to $[PhBP_3^{Ph}]Fe$.[34] That no net reaction is observed upon *in situ* reduction of $[PhBP_3^{mter}]FeCl$ under $CO_2$ strongly suggests that, even if $CO_2$ binds weakly to the iron(I) state, a bimolecular pathway is required to go on to a stable product. Our spectroscopic efforts to observe a "$[PhBP_3^R]Fe(CO_2)$" adduct species were unsuccessful, even at very low temperatures.

The aforementioned discussion collectively suggests that a sterically accessible iron(I) center is required to facilitate the reductive coupling pathway. When this requirement is not met, decarbonylation to generate bridging oxo species (**2**, **10**, **12**) instead occurs. That no decarbonylation is observed in the reaction between *in situ* generated $[PhBP_3^{mter}]Fe$(I) and $CO_2$ suggests that the irreversible C–O bond cleavage step involves two iron centres. Such decarbonylation reactions are well precedented for early transition metals,[39] with fewer well-defined examples for mid-to-late transition metals.[40]

### III.2 Role of solvent in $CO_2$ reductive coupling

The ability of $[PhBP_3^{CH_2Cy}]Fe(PR'_3)$ to reduce $CO_2$ to give either oxalate **3** or the partial decarbonylation product **2** is solvent dependent. Thus, in both benzene and THF, reductive coupling to give oxalate occurs preferentially over reductive cleavage (Table 1). This contrasts with the reactivity in MeCy, in which reductive cleavage is exclusively observed. The solvent dependence of the reaction could be attributed to: (i) variable solubility of $CO_2$ in the solvents employed, (ii) variable solvent polarity, or (iii) differences in the ability of the solvents to coordinate iron(I).

We do not think that the variable solubility of $CO_2$ in the solvents canvassed plays a substantive role in the product profiles observed. Were it to do so, we might expect the product distribution of the reaction between $PPh_3$-capped **7** and $CO_2$ in various solvents to mirror the solubility of $CO_2$ in these solvents. Under the assumption that the Henry's law constant for $CO_2$ in *n*-heptane is similar to that of MeCy and that for toluene is similar to that of benzene, the solubility of $CO_2$ should increase in the order: THF < MeCy < benzene (Henry's law constants at 25 °C for THF, *n*-heptane, and toluene are 44.9, 84.0, and 98.1 $atm^{-1}$, respectively).[27] If $CO_2$ solubility were dictating the reaction outcome for the reaction between **7** and $CO_2$, then a distinct product profile would be observed in THF relative to that in benzene and MeCy. This is not the case, as the reaction in MeCy is distinct from that in benzene and also that in THF. While this argument is overly simplistic, the modest differences in $CO_2$ solubility in the three solvents canvassed do not likely dominate the outcome of the reaction.

The product profiles observed in the aforementioned solvents for the reaction of **7** and $CO_2$ are likewise not consistent with solvent polarity dictating the product profile. Using the static dielectric constants for THF (7.32), benzene (2.28), and MeCy (2.02)[41] as a means to gauge solvent polarity, it is anticipated that the reaction in THF should be distinct from that in benzene and MeCy. Yet this is not the case, as the product profile observed in MeCy differs dramatically from that observed in THF and benzene.

To determine the role that solvent coordination may have on the product profile, the reaction between **8** and $CO_2$ was carried out in THF, 2-methyl-THF and 2,5-dimethyl-THF.[28] The product profile of these reactions could then be compared with that of the reaction run in MeCy. The relative amounts of **2** and **3** formed in the reaction between **8** and $CO_2$ gradually changes as a function of THF *vs.* 2-methyl-THF *vs.* 2,5-dimethyl-THF, solvents of comparable dielectric constants (see Fig. 2 for comparative IR spectra). Most strikingly, the product profile in 2,5-dimethyl-THF more closely mirrors that in MeCy than in THF. Given that the coordinating affinities of these solvents should obey the trend THF > 2-methyl-THF > 2,5-dimethyl-THF due to their steric profiles,[28] we highlight solvent coordination at iron as the key factor causing the marked solvent dependence on the product profile between iron(I) and $CO_2$ in the $[PhBP_3^{CH_2Cy}]Fe$ system. When solvent cannot coordinate, the decarbonylation pathway is clearly favoured.

A plausible mechanistic scenario is shown in Scheme 6 whereby the radical coupling reaction to give μ-oxalate **3** ensues from an electronically saturated iron complex; the iron is oxidized to iron(II) as the $CO_2$ is reduced by one electron, priming it for reductive coupling. Coordination of two THF solvent ligands and $CO_2$ to an Fe(I) center would afford a formally 19-electron complex, $[PhBP_3^{CH_2Cy}]Fe(\eta^1\text{-}OCO)(THF)_2$, in which the unpaired electron would be delocalized from the iron center onto the coordinated $CO_2$ ligand. Consistent with this notion, a DFT minimized structure of the 19-electron species $[PhBP_3^{Me}]Fe(\eta^1\text{-}OCO)(THF)_2$ (where the ligand has been truncated owing to difficulties minimizing the MeCy system) features 77% of the spin-density on the $CO_2$ carbon atom (in contrast, the

 

spin-density on lower electron count 4- and 5-coordinate species is predominantly iron centred; see ESI†). C–C coupling from an intermediate such as $[PhBP_3^{CH_2Cy}]Fe(\eta^1\text{-}OCO)(THF)_2$ would account for the generation of **3** (with concomitant loss of the coordinated THF). This idea draws parallels to the reductive coupling of benzene known to be mediated by 19-electron metal species,[18a] as is observed in the present system (*vide supra*, Section II.2). The reactivity of azobenzene with **1** is likewise conceptually similar. By contrast, the reaction to give μ-O/μ-CO **2** is suggested to occur from a lower coordinate (hence lower valence electron count) iron center.

Reductive coupling of $CO_2$ is only observed for the least sterically encumbering ancillary ligand, which we suspect is due to more favourable solvation of the $CO_2$ adduct (binding of up to two L-type solvent molecules). Hence, no oxalate species is obtained in the reactions of either $[PhBP_3^{iPr}]Fe$ or $[PhBP_3^{Ph}]Fe$ with $CO_2$. Additionally, solvation would add steric protection at each iron center, disfavouring the formation of dimeric intermediates and products. Though both **2** and **3** are dimeric species, the production of **2** should show a much stronger steric limitation owing to its very short Fe–Fe distance (2.384(4) Å) by comparison to the very long Fe–Fe distance in **3** (5.343(4) Å). The coupling reaction to generate **3** presumably occurs between two $CO_2$-centered radicals that are spatially well separated from the iron centres, as inferred from the structure of μ-oxalate **3**. In contrast, we postulate that the reaction to generate μ-O/μ-CO **2** likely occurs between the iron center of **1** and the coordinated $CO_2$ of **1**-$CO_2$. The added bulk induced by coordination of either one or two molecules of THF solvent would have a more pronounced effect on the rate of formation **2**. It should be emphasized that $[PhBP_3^{CH_2Cy}]Fe(CO_2)(solv.)_x$ intermediates of the types shown in Scheme 6 are suggested to account for the respective reactivity profiles. Attempts to spectroscopically observe such intermediates by VT-NMR or VT-react-IR have been unfruitful.

In coordinating solvents, a 19-electron species of the type $[PhBP_3^{CH_2Cy}]Fe(\eta^1\text{-}OCO)(THF)_2$ (in THF) or $[PhBP_3^{CH_2Cy}]Fe(\eta^1\text{-}OCO)(\eta^4\text{-}C_6H_6)$ (in benzene) may undergo C–C coupling from such an intermediate to account for formation of μ-oxalate **3**. Though never directly observed in oxalate forming systems, $M(\eta^1\text{-}OCO)$ species of this type[42] have been invoked in other systems that couple $CO_2$ to oxalate.[10b] In the absence of coordinating solvents or owing to solvent lability, 15- or 17-electron $CO_2$ adduct intermediates are likely. Though these species are drawn as $\eta^2$-*O*CO adducts of iron in Scheme 6, the DFT calculations (see ESI†) suggest that both $\eta^1$-*O*CO and $\eta^2$-*O*CO species may be viable intermediates. Such species would bimolecularly react with a second equivalent of iron(I) to give the decarbonylation product **2**.

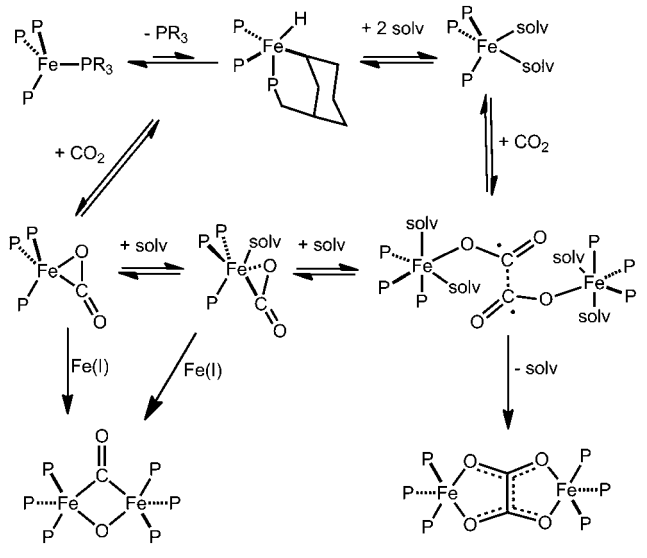


Scheme 6

## IV Conclusions

To achieve selectivity for either formation of the partial decarbonylation product μ-O/μ-CO **2** or the $CO_2$-coupling product **3**, synthetic strategies have been successfully implemented motivated by our initial hypothesis that the ratio of reactive **1** *vs.* $CO_2$ in solution would impact the product distribution. These synthetic approaches proved practical for controlling the effective concentrations of the active iron(I) species relative to $CO_2$ in solution, and thereby exposed the role that the reaction solvent and also the ancillary ligand (*i.e.*, $[PhBP_3^R]^-$; R = Ph, $^i$Pr, $CH_2Cy$, *m*ter; *m*ter = 3,5-*meta*-terphenyl) had on the product distribution. We have determined that reductive coupling to oxalate only occurs with the "$[PhBP_3^{CH_2Cy}]Fe(I)$" platform and that this $CO_2$-coupling product is preferred in a solvent that can coordinate the iron center. We presume spin leakage onto $CO_2$ occurs under such a scenario. Empirically we find that in THF $CO_2$ coupling to μ-oxalate **3** is favoured, whereas in methylcyclohexane (MeCy) partial decarbonylation to generate μ-O/μ-CO **2** occurs exclusively. Our studies underscore the ability to tune reaction conditions such that the $CO_2$ product distribution is altered in the presence of iron(I).

## Acknowledgements

This work was generously supported by the NSF (CHE-0750234) and the Gordon and Betty Moore Foundation. C. T. S. is grateful for an NSF graduate fellowship. We are also grateful to the Massachusetts Institute of Technology, Cambridge, Massachusetts, 02139, where some of the research described was conducted.

## Notes and references

1 (*a*) T. Sakakura, J.-C. Choi and H. Yasuda, *Chem. Rev.*, 2007, **107**, 2365–2387; (*b*) P. Braunstein, D. Matt and D. Nobel, *Chem. Rev.*, 1988, **88**, 747–764; (*c*) M. Aresta and A. Dibenedetto, *Dalton Trans.*, 2007, 2975–2992; (*d*) H. Arakawa, M. Aresta, J. N. Armor, M. A. Barteau, E. J. Beckman, A. T. Bell, J. E. Bercaw, C. Creutz, E. Dinjus, D. A. Dixon, K. Domen, D. L. DuBois, J. Eckert, E. Fujita, D. H. Gibson, W. A. Goddard, D. W. Goodman, J. Keller, G. J. Kubas, H. H. Kung, J. E. Lyons, L. E. Manzer, T. J. Marks, K. Morokuma, K. M. Nicholas, R. Periana,

L. Que, J. Rostrup-Nielson, W. M. H. Sachtler, L. D. Schmidt, A. Sen, G. A. Somorjai, P. C. Stair, B. R. Stults and W. Tumas, *Chem. Rev.*, 2001, **101**, 953–996; (*e*) E. E. Benson, C. P. Kubiak, A. J. Sathrum and J. M. Smieja, *Chem. Soc. Rev.*, 2009, **38**, 89–99; (*f*) K. Huang, C.-L. Sun and Z.-J. Shi, *Chem. Soc. Rev.*, 2011, **40**, 2435–2452.

2 N. M. West, A. J. M. Miller, J. A. Labinger and J. E. Bercaw, *Coord. Chem. Rev.*, 2011, **255**, 881–898.

3 (*a*) D. J. Darensbourg, *Chem. Rev.*, 2007, **107**, 2388–2410; (*b*) M. Cheng, E. B. Lobkovsky and G. W. Coates, *J. Am. Chem. Soc.*, 1998, **120**, 11018–11019.

4 C. S. Yeung and V. M. Dong, *J. Am. Chem. Soc.*, 2008, **130**, 7826–7827.

5 (*a*) O. Vechorkin, N. Hirt and X. Hu, *Org. Lett.*, 2010, **12**, 3567–3569; (*b*) I. I. F. Boogaerts and S. P. Nolan, *J. Am. Chem. Soc.*, 2010, **132**, 8858–8859.

6 C. Amatore and J. M. Saveant, *J. Am. Chem. Soc.*, 1981, **103**, 5021–5023.

7 J.-M. Savéant, *Chem. Rev.*, 2008, **108**, 2348–2378.

8 A. Mendiratta and C. C. Cummins, *Inorg. Chem.*, 2005, **44**, 7319–7321.

9 (*a*) W. J. Evans, C. A. Seibel and J. W. Ziller, *Inorg. Chem.*, 1998, **37**, 770–776; (*b*) W. J. Evans, S. E. Lorenz and J. W. Ziller, *Inorg. Chem.*, 2009, **48**, 2001–2009; (*c*) D. M. Y. Barrett Adams, I. A. Kahwa and J. T. Mague, *New J. Chem.*, 1998, **22**, 919–921.

10 (*a*) L. J. Farrugia, S. Lopinski, P. A. Lovatt and R. D. Peacock, *Inorg. Chem.*, 2000, **40**, 558–559; (*b*) R. Angamuthu, P. Byers, M. Lutz, A. L. Spek and E. Bouwman, *Science*, 2010, **327**, 313–315.

11 M. Aresta, R. Gobetto, E. Quaranta and I. Tommasi, *Inorg. Chem.*, 1992, **31**, 4286–4290.

12 C. C. Lu, C. T. Saouma, M. W. Day and J. C. Peters, *J. Am. Chem. Soc.*, 2007, **129**, 4–5.

13 A. Klose, J. Hesschenbrouck, E. Solari, M. Latronico, C. Floriani, N. Re, A. Chiesi-Villa and C. Rizzoli, *J. Organomet. Chem.*, 1999, **591**, 45–62.

14 H. O. Froehlich and H. Schreer, *Zeitschrift für Chemie*, 1983, **23**, 348.

15 A. M. Gaffney, J. J. Leonard, J. A. Sofranko and H. N. Sun, *J. Catal.*, 1984, **90**, 261–269.

16 (*a*) I. Bhugun, D. Lexa and J. M. Saveant, *J. Am. Chem. Soc.*, 1996, **118**, 1769–1776; (*b*) B. Fisher and R. Eisenberg, *J. Am. Chem. Soc.*, 1980, **102**, 7361–7363; (*c*) J. P. Collin, A. Jouaiti and J. P. Sauvage, *Inorg. Chem.*, 1988, **27**, 1986–1990.

17 (*a*) K. Jonas, G. Koepe, L. Schieferstein, R. Mynott, C. Krüger and Y.-H. Tsay, *Angew. Chem., Int. Ed. Engl.*, 1983, **22**, 620–621; (*b*) G. Bai, P. Wei and D. W. Stephan, *Organometallics*, 2005, **24**, 5901–5908; (*c*) W. V. Konze, B. L. Scott and G. J. Kubas, *J. Am. Chem. Soc.*, 2002, **124**, 12550–12556; (*d*) J. C. Thomas and J. C. Peters, *J. Am. Chem. Soc.*, 2003, **125**, 8870–8888.

18 (*a*) D. Astruc, *Chem. Rev.*, 1988, **88**, 1189–1216; (*b*) J. R. Hamon, D. Astruc and P. Michaud, *J. Am. Chem. Soc.*, 1981, **103**, 758–766.

19 (*a*) S. D. Grumbine, R. K. Chadha and T. D. Tilley, *J. Am. Chem. Soc.*, 1992, **114**, 1518–1520; (*b*) B. W. Cohen, D. E. Polyansky, R. Zong, H. Zhou, T. Ouk, D. E. Cabelli, R. P. Thummel and E. Fujita, *Inorg. Chem.*, 2010, **49**, 8034–8044.

20 (*a*) B. A. Frazier, P. T. Wolczanski, E. B. Lobkovsky and T. R. Cundari, *J. Am. Chem. Soc.*, 2009, **131**, 3428–3429; (*b*) T. R. Dugan, E. Bill, K. C. MacLeod, G. J. Christian, R. E. Cowley, W. W. Brennessel, S. Ye, F. Neese and P. L. Holland, *J. Am. Chem. Soc.*, 2012, **134**, 20352–20364.

21 (*a*) E. B. Hulley, P. T. Wolczanski and E. B. Lobkovsky, *J. Am. Chem. Soc.*, 2011, **133**, 18058–18061; (*b*) C. C. Hojilla Atienza, C. Milsmann, S. P. Semproni, Z. R. Turner and P. J. Chirik, *Inorg. Chem.*, 2013, **52**, 5403–5417.

22 (*a*) S. Gambarotta, C. Floriani, A. Chiesi-Villa and C. Guastini, *J. Am. Chem. Soc.*, 1983, **105**, 7295–7301; (*b*) B. Hansert and H. Vahrenkamp, *J. Organomet. Chem.*, 1993, **459**, 265–269; (*c*) A. D. Ryabov, L. G. Kuz'mina, N. V. Dvortsova, D. J. Stufkens and R. van Eldik, *Inorg. Chem.*, 1993, **32**, 3166–3174; (*d*) Y. Miyaki, T. Onishi and H. Kurosawa, *Chem. Lett.*, 2000, **29**, 1334–1335.

23 (*a*) L. D. Field, H. L. Li, S. J. Dalgarno and P. Turner, *Chem. Commun.*, 2008, 1680–1682; (*b*) A. R. Sadique, E. A. Gregory, W. W. Brennessel and P. L. Holland, *J. Am. Chem. Soc.*, 2007, **129**, 8112–8121; (*c*) R. S. Dickson and J. A. Ibers, *J. Am. Chem. Soc.*, 1972, **94**, 2988–2993.

24 J. J. de Lange, J. M. Robertson and I. Woodward, *Proc. R. Soc. London, Ser. A*, 1939, **171**, 398–410.

25 S. D. Brown, T. A. Betley and J. C. Peters, *J. Am. Chem. Soc.*, 2003, **125**, 322–323.

26 (*a*) E. J. Daida and J. C. Peters, *Inorg. Chem.*, 2004, **43**, 7474–7485; (*b*) C. T. Saouma and J. C. Peters, *Coord. Chem. Rev.*, 2011, **255**, 920–937.

27 A. Gennaro, A. A. Isse and E. Vianello, *J. Electroanal. Chem.*, 1990, **289**, 203–215.

28 M. J. Wax and R. G. Bergman, *J. Am. Chem. Soc.*, 1981, **103**, 7028–7030.

29 D. F. Aycock, *Org. Process Res. Dev.*, 2006, **11**, 156–159.

30 T. A. Betley and J. C. Peters, *J. Am. Chem. Soc.*, 2003, **125**, 10782–10783.

31 K. Schwabe and G. Gebhardt, *Z. Anorg. Allg. Chem.*, 1954, **277**, 329–340.

32 T. A. Betley and J. C. Peters, *Inorg. Chem.*, 2003, **42**, 5074–5084.

33 (*a*) C. Fernandes, A. Neves, A. J. Bortoluzzi, B. Szpoganicz and E. Schwingel, *Inorg. Chem. Commun.*, 2001, **4**, 354–357; (*b*) M. K. Reinking, J. Ni, P. E. Fanwick and C. P. Kubiak, *J. Am. Chem. Soc.*, 1989, **111**, 6459–6461.

34 C. T. Saouma, C. C. Lu and J. C. Peters, *Inorg. Chem.*, 2012, **51**, 10043–10054.

35 K. Nakamoto, *Infrared and Raman Spectra of Inorganic and Coordination Compounds Part B: Applications in Coordination, Organometallic, and Bioinorganic Chemistry*, John Wiley & Sons, Inc., New York, 1997.

36 N. A. Eckert, S. Stoian, J. M. Smith, E. L. Bominaar, E. Münck and P. L. Holland, *J. Am. Chem. Soc.*, 2005, **127**, 9344–9345.

37 S. D. Brown and J. C. Peters, *J. Am. Chem. Soc.*, 2005, **127**, 1913–1923.

38 C. A. Tolman, *Chem. Rev.*, 1977, **77**, 313–348.

 

39 (*a*) G. Fachinetti, C. Floriani, A. Chiesivilla and C. Guastini, *J. Am. Chem. Soc.*, 1979, **101**, 1767–1775; (*b*) C. Bianchini and A. Meli, *J. Am. Chem. Soc.*, 1984, **106**, 2698–2699; (*c*) J. C. Bryan, S. J. Geib, A. L. Rheingold and J. M. Mayer, *J. Am. Chem. Soc.*, 1987, **109**, 2826–2828.

40 (*a*) D. S. Laitar, P. Müller and J. P. Sadighi, *J. Am. Chem. Soc.*, 2005, **127**, 17196–17197; (*b*) J. W. Raebiger, J. W. Turner, B. C. Noll, C. J. Curtis, A. Miedaner, B. Cox and D. L. DuBois, *Organometallics*, 2006, **25**, 3345–3351; (*c*) M. Rakowski Dubois and D. L. Dubois, *Acc. Chem. Res.*, 2009, **42**, 1974–1982; (*d*) A. R. Sadique, W. W. Brennessel and P. L. Holland, *Inorg. Chem.*, 2008, **47**, 784–786.

41 A. J. Gordon and R. A. Ford, *The Chemist's Companion: A Handbook of Practical Data, Techniques, and References*, Wiley-Interscience Publication, 1972.

42 (*a*) I. Castro-Rodriguez, H. Nakai, L. N. Zakharov, A. L. Rheingold and K. Meyer, *Science*, 2004, **305**, 1757–1760; (*b*) M. Fang, J. H. Farnaby, J. W. Ziller, J. E. Bates, F. Furche and W. J. Evans, *J. Am. Chem. Soc.*, 2012, **134**, 6064–6067.